Title
K""INTERACTIONS IN DEUTERIUM

Authors
Dahl, O.
Horwitz, N.
Miller, D.
et al.

Publication Date
1960-08-01

UCRL 8135

UNIVERSITY OF CALIFORNIA

Ernest O. Lawrence

Radiation Laboratory

BERKELEY, CALIFORNIA

DISCLAIMER

for pub Health Physics

UCRL-8735

UNIVERSITY OF CALIFORNIA
Lawrence Radiation Laboratory
Berkeley, California

Contract No. W-7405-eng-48

A HIGH-ENERGY NEUTRON DOSIMETER

Joseph B. McCaslin

April 21, 1959

Printed for the U. S. Atomic Energy Commission

A HIGH-ENERGY NEUTRON DOSIMETER

Joseph B. McCaslin

Lawrence Radiation Laboratory
University of California
Berkeley, California

April 21, 1959

ABSTRACT

High-energy neutrons and protons in the range 20.4 Mev to more than 400 Mev can be detected in 1720-gram plastic scintillators by means of (n, 2n) and (p, pn) reactions with carbon nuclei. Carbon-11 is formed which emits positrons of E_{max} = 0.98 Mev and has a half life of 20.4 min. With scintillators irradiated to saturation in a neutron flux density of 1 neutron $cm^{-2} sec^{-1}$, a subsequent 5-minute waiting period, and a 38-minute counting time, the standard deviation in the counting statistics is less than 15%. Background considerations are discussed along with some experimental and theoretical values of the (n, 2n) reaction cross sections.

A HIGH-ENERGY NEUTRON DOSIMETER*

Joseph B. McCaslin

Lawrence Radiation Laboratory
University of California
Berkeley, California

April 21, 1959

I. INTRODUCTION

A dosimeter in which both neutrons and protons are detected covers the energy region from 20.4 Mev[1] to more than 400 Mev. The method of detection involves the production of carbon-11 from carbon-12 by (n, 2n) and (p, pn) reactions with carbon nuclei. Carbon-11 is a positron emitter of E_{max} = 0.98 Mev. The half life is 20.4 minutes, and there are no significant competing reactions. The (n, 2n) reaction cross sections are fairly constant above about 50 Mev.

Carbon in the form of plastic scintillator material is used as the detector. These scintillators (see Fig. 1) are 5 inches in diameter and 5 inches high, and weigh 1720 grams each. Not only is the energy of the positron expended entirely in the scintillator, but the energy of one or both of the annihilation gammas is likewise largely contained.

---

*Work done under the auspices of the U. S. Atomic Energy Commission.

II. COUNTING SYSTEM

The scintillators are placed in an area to be monitored and exposed for a suitable period of time (preferably to saturation, for low flux densities), and are then removed to an area of lower background for counting. As with other threshold detectors, this method enjoys the advantage of being insensitive to accelerator-produced gamma rays.

These scintillators are counted in a mineral oil bath on top of a vertically mounted Du Mont 6364 photomultiplier, as shown in Fig. 2. The lighttight housing for the photomultiplier consists of a mild steel box 20 inches high, 8 inches on each side, and 1/4 inch thick (see Fig. 3). Mild steel was chosen because of its value as a magnetic shield, since on occasion C^{11} has been counted near the Bevatron. In addition to the lid on top, there is another opening on the side, near the bottom, for access to the phototube base.

A white paint, Kerpro No. 22 (titanium dioxide pigment in a clay base), was used to spray all but the viewing end of each scintillator. Figure 4 shows how painting the scintillator increased the gain, as indicated by the lower setting of the high voltage. The curves are differential pulse-height distributions from a Co^{60} source.

Pulses from the photomultiplier are fed to a preamplifier, after which they are clipped so that all pulses have a uniform width of 2 microseconds. The pulses are then fed into a UCRL Model 5 linear amplifier, from there to an Atomic single-channel pulse-height analyzer, and then to a scaler. See Fig. 5. The resolving time of the entire system is less than 5 microseconds. It is necessary to gate the scalers off during the acceleration phases of the Bevatron and 184-inch cyclotron cycles even though the counting equipment is normally located some distance away. Bevatron gating is accomplished through the use of a telemetering unit which produces a gating pulse at the start of the Bevatron acceleration cycle. This pulse is fed into a variable gate and delay chassis where it is shaped and stretched to form a 3-second-long off gate. A 1000-cycle pulse-generator signal is fed into a similarly gated scaler in order to keep track of counting time. A cyclotron triggering signal is run directly into a variable gate and delay chassis and is treated in a similar manner except that the off gates are

only a few milliseconds long. However, the repetition rate is high, about 63 pulses per second. The loss of counting time due to gating is considerable and is a matter of great concern. The data treatment presented here presupposes no losses of this kind. Often something less than this ideal is realized in practice.

III. BACKGROUND

The counting equipment is located in a small building which has 1-foot-thick heavy aggregate concrete walls. The photomultiplier housing is surrounded by 4 inches of lead. No significant difference was noted when 4 more inches of lead was added. Photomultiplier noise, measured with scintillator removed, did not add appreciably to the background, therefore it was not considered necessary to view both ends of the scintillator with two phototubes in coincidence.

The 1/16 inch of lead used to line the inside walls of the photomultiplier housing greatly reduced the background, especially in the low-level channels. Background was reduced by a factor of 0.56 between 5 and 10 volts, and 0.91 between 20 and 25 volts.

At first it was felt that in addition to the cosmic-ray background there might be a significant portion of the total background due to high-energy gamma rays produced by thermal-neutron capture in either the lead shielding or the iron wall. This was shown not to be an important factor at the present background levels: the background counting rate did not decline when boron-loaded paraffin blocks were stacked around the photomultiplier house.

In an attempt to further reduce background, a cosmic-ray anticoincidence shield was employed. A piece of plastic scintillator 1 inch thick and 13 inches in diameter, viewed by two photomultipliers, was placed over the photo-multiplier house. Background was reduced by this method, but only by 10%, which at this stage of development did not in the author's estimation warrant the time that would be necessary to properly maintain the anti-coincidence system. Certainly, some of the low-activity construction materials, mercury shielding, quartz window phototubes etc., would do much to further reduce background. Figure 6 shows the present state of the background.

A system similar to that used for counting C^{11} has been used simultaneously with the C^{11} system in order to check background during counting of the activated scintillator.

IV. COUNTING CONSIDERATIONS AND STATISTICS

Since accelerator-produced gamma rays are not counted, extrapolation of the integral bias curve is greatly facilitated because there is no confusion between these gammas and small C^{11}- produced pulses near the zero-bias intercept. The shape of the integral bias curves was determined from high-level activations in order that an accurate correction factor for the extrapolation to zero bias could be obtained. Pulses were taken from 5 to 45 volts in 5-volt steps and then corrected for saturation, decay, and background. It will be noted from Fig. 7 that the shapes of the integral bias curves obtained from two different scintillators under different beam intensities and corrected for decay become rather flat as the zero-bias intercept is approached. If many counts were being lost the curves would be more steep in this region. Normally, it should not be necessary to make corrections for individual scintillators. For the two curves shown the zero-bias correction factors are within 5% at 10 volts. Integral counts are taken at the 10-volt point, since from examination of the C^{11} and background curves the ratio of the standard deviation of the total count to the C^{11} count is a minimum at this point.

Calculation of Induced Activity

At saturation we have

$$\frac{dN}{dt} = nv\sigma_{(n, 2n)}Nt = -\frac{dN'}{dt}, \qquad (1)$$

where

$\frac{dN}{dt}$ = C^{11} production rate,

nv = neutron flux density,

$\sigma_{(n, 2n)}$ = neutron absorption cross section leading to the production of positron activity,

Nt = total number of C^{12} atoms,

$= 7.88 \times 10^{25}$ atoms C^{12} per scintillator,

$\frac{dN'}{dt}$ = zero-time disintegration rate.

If an incident neutron flux density of 1 neutron $cm^{-2} sec^{-1}$ and a cross section of $22 \cdot 10^{-27} cm^2$ is assumed, we find

$$\frac{dN'}{dt} = 104 \text{ disintegrations per minute.}$$

After a 5-minute delay prior to counting there would be

$$\frac{dN'}{dt} \left(e^{\frac{-tw}{T}} \right) = 87.7 \text{ dpm,}$$

where T = mean life of C^{11},

tw = delay time prior to counting.

Of these, 92% possess sufficient height to overcome the lower level bias and be counted.

The counting errors were computed as follows:

$$Nd = C \int_{tw}^{tw+tc} (dN/dt)\, dt = C \int_{tw}^{tw+tc} R_0 e^{\frac{-t}{T}} dt \qquad (2)$$

$$= R_0 TC \left[e^{\frac{-tw}{T}} - e^{-\left(\frac{tw+tc}{T}\right)} \right], \qquad (3)$$

where Nd = number of disintegrations occurring during the counting period after secular equilibrium has been reached,

R_0 = initial decay rate of the scintillator upon removal from the neutron flux,

T = mean life,

C = zero-bias correction factor,

t_w = initial decay time prior to counting,

t_c = counting time.

It is assumed that no time is lost by gating, and that the scintillator did not undergo changes in the incident flux level during irradiation. Then,

$$\text{percent standard deviation} = \frac{\left[(\sqrt{Nd + Btc})^2 + (\sqrt{Btc})^2\right]^{1/2} \times 100}{Nd}, \quad (4)$$

where B is the background in cpm,
which simplifies to

$$\text{percent standard deviation} = \frac{100\sqrt{Nd + 2\,B\,tc}}{Nd} = \sigma. \quad (5)$$

The optimum counting times for minimum standard deviations may be computed by differentiating Eq. (5) and finding, for various values of R_0, the value of t_c that satisfies the equation $d\sigma/dtc = 0$,

$$0 = 1 - \left[e^{\frac{tc}{T}}\right] + \left[\frac{K}{2BT} e^{\frac{-tw}{T}}\right] + \left[\frac{2t_c}{T}\right] - \left[\frac{K}{2TB} e^{\frac{-(tw+tc)}{T}}\right], \quad (6)$$

where $K = R_0TC$.

Figure 8 is a special case of Eq. (5) and shows the error associated with the count as a function of the counting time for an incident flux density of 1 neutron cm^{-2} sec^{-1} for a scintillator irradiated to saturation, and including a 5-minute decay period prior to counting. Five minutes or less is usually sufficient time for transporting the scintillator to the counting area. For an optimum counting time of 38 minutes, this neutron-flux density can be determined with a standard deviation of 14.5%. Optimum counting times for other neutron flux densities were calculated from Eq. (6) and shown in Fig. 9. These values of time and flux density were then substituted in Eq. (5) and the corresponding values of percent standard deviation were plotted versus neutron flux density in Fig. 10. Thus a flux density of 20 $n/cm^2/sec$ can be determined with an error of less than 1% when a counting time of 48 minutes is used. These figures are standard deviations based on counting statistics and do not include systematic errors or errors in the determination of the reaction cross section.

An interesting method of further increasing the sensitivity of the system might consist of an upper-level discriminator set at 1.5 or 2 Mev.[2]

In effect, then, one would have a single-channel differential pulse-height analyzer with a very large window. Advantage is taken of the fact that the integral bias curve for C^{11} falls off rapidly at these energies, while the background curve is still relatively flat. Figure 11 shows the minimum percent standard deviations as a function of window width at various bias levels for these differential counts. A neutron flux density of 1 $n/cm^2/sec$, secular equilibrium, a 5-minute decay, and a 40-minute counting time were assumed. Thus, for a window looking between 20 and 50 volts, (a window width of 30 v, and a 20-v bias) a minimum standard deviation of 13% may be realized.

The graph shown in Fig. 12 is a plot of % saturation vs irradiation time,

$$\% \text{ saturation} = 100(1 - e^{-t/T}) \tag{7}$$

where t = irradiation time, which may facilitate calculations involving irradiations other than those producing saturated activity. An uninterrupted uniform irradiation rate over the entire exposure period is assumed.

In this case we have

$$Nd = K R_0 TC \left[\exp\left(-\frac{tw}{T}\right) - \exp\left(-\frac{tw+tc}{T}\right)\right], \tag{8}$$

where K = % saturation/100.

Figure 13 presents an easy method of determining the amount of activity remaining following waiting periods (t_w) other than the 5-minute value used in the calculations.

V. REACTION CROSS SECTIONS

The cross section as a function of energy of the $C^{12}(p, pn)C^{11}$ reaction has been reported in a number of papers and is well known.[3] (See Fig. 14). Data on the $C^{12}(n, 2n)C^{11}$ reaction cross section have been determined for only a few energies; however, at high energies the cross section should be proportional to the nucleon-nucleon cross section. Based on the data in Figs. 15 and 16 for neutron-neutron and proton-neutron cross sections at high energies,[4] an approximation of the (n, 2n) cross section has been made.[5] We have

$$\frac{\sigma(n, 2n)}{\sigma(p, pn)} \propto \frac{N\sigma(n, n)}{N\sigma(p, n)} = \frac{6(24)}{6(36)} = \frac{2}{3} \text{ at 300 Mev,}$$

where N is the number of neutrons in the carbon nucleus. This ratio, determined for several energies, is applied as a correction factor to the better-known (p, pn) cross sections at corresponding energies. Thus, at 300 Mev the (n, 2n) cross section has been estimated to be 24 millibarns.

Also theoretically, on the flat portion of the excitation curve, the yield should be less for neutrons than for protons if exchange collisions occur. This is because a (p, n) exchange can lead to C^{11} by proton evaporation, but an (n, p) exchange cannot lead to C^{11}.[6]

No attempt has been made in the calculations to correct for this process. The calculated values for the (n, 2n) cross sections should be viewed as approximations, and are more applicable above 100 Mev. However, the cross section has been measured for 90-Mev neutrons;[6] the results of three consecutive measurements are 21, 24, and 22 ± 4.0 mb. In another, more recent, report on a similar system using liquid scintillator, a cross section of 21 to 22 mb was used for neutron energies greater than 40 Mev; however, no reference for these values was cited.[7]

Near the (n, 2n) reaction threshold, the cross section should be proportional to the square root of the energy excess.[8] The values of about 4.5 mb and 10 mb at approximately 23.5 and 27.5 Mev respectively[8] are consistent with theory.

Whether or not there is a peak in the (n, 2n) reaction cross section in the region of 40 Mev involves the importance of "intermediate-nucleus" reactions in relation to noncapture processes.[6] No such evaluations are

included in this report; however, if such a peak exists, it will lead to an overestimation of the neutron flux density in this region.

In the region 22 ± 4 Mev there is a sharp (γ, n) resonance leading to the production of C^{11}.[10] The (γ, n) reaction cross section is on the order of 8 mb. At higher energies this cross section is down by two orders of magnitude. More than 60% of these high-energy gammas will be absorbed in 1 cm of lead, thus serving as an easy check on the importance of this reaction as a possible source of error.

VI. CONCLUDING REMARKS

When not used for C^{11} counting, the system has been used for counting other threshold detectors, and, in conjunction with a NaI(Tl) crystal, for gamma-ray spectroscopy. Iron, aluminum, and nickel sleeves are activated and placed around either a 4.5×4.5-inch-diameter NaI crystal or a plastic scintillator (Figs. 17 and 18). The incident neutron flux is then determined either by observing the activity under the photopeak with the NaI, or by observing the total activity with a plastic scintillator. Work is currently in progress to determine ways of utilizing these other threshold detectors to best advantage.[11]

Figures 19 and 20 illustrate the difference in energy resolution between the plastic scintillators and a 3×3-inch NaI(Tl) crystal. The curves show the differential pulse-height distributions from a Na^{22} source. The energy resolution of the system (full width at half maximum) with the NaI is 15% and 8% respectively on the two peaks. While such a system for C^{11} counting is being set up, a multichannel analyzer is of great assistance, but once it is set up a single discriminator is adequate. Gain is periodically checked by placing a gamma source in some standard geometry and making the necessary adjustments to produce a standard counting rate above the discriminator setting.

To summarize, a sensitive method of detecting high-energy neutrons and protons in the range 20 Mev to more than 400 Mev has been constructed with a counting error less than 15% for flux densities of 1 neutron $cm^{-2} sec^{-1}$. Further experimental verification of the (n, 2n) cross section would be desirable; however, sufficient information is available for most survey purposes.

ACKNOWLEDGMENTS

The work presented in this report involved the help, advice, and cooperation of the entire Health Physics Group.

In particular the author wishes to thank Professor Burton J. Moyer, Dr. Roger W. Wallace, H. Wade Patterson, Lloyd D. Stephens, and T. M. Jenkins. The assistance of Dr. Wilmot N. Hess was invaluable in the preparation of the section on reaction cross sections.

A large share of the work, planning, and evaluation was performed with the direct assistance of Alan R. Smith, for whose contributions the author is indeed grateful.

References

1. J. Sharpe and G. H. Stafford, Proc. Phys. Soc. A64, 211 (1951).
2. Alan R. Smith (Lawrence Radiation Laboratory) private communication.
3. Crandall, Milburn, Pyle, and Birnbaum, Phys. Rev. 101, 329 (1956).
4. Wilmot N. Hess, Revs. Modern Phys. 30, No. 2, 368-401 Apr. (1958).
5. Wilmot N. Hess, (Lawrence Radiation Laboratory) private communication.
6. E. M. McMillan and H. F. York, Phys. Rev. 73, 262 (1948).
7. P. S. Baranov and V. I. Gol'danskii, Rev. Sci. Instr. 28, No. 12, 1029 Dec. 1957.
8. E. Fermi, Nuclear Physics course notes compiled by Jay Orear, A. H. Rosenfeld, and R. A. Schluter (Univ. of Chicago Press, Chicago, 1950), p. 144.
9. Brolley, Fowler and Schlacks, Phys. Rev. 88, 618 (1952).
10. Barker, George, and Reagan, Phys. Rev. 98, 73 (1955).
11. T. M. Jenkins, (Lawrence Radiation Laboratory, work in progress.)

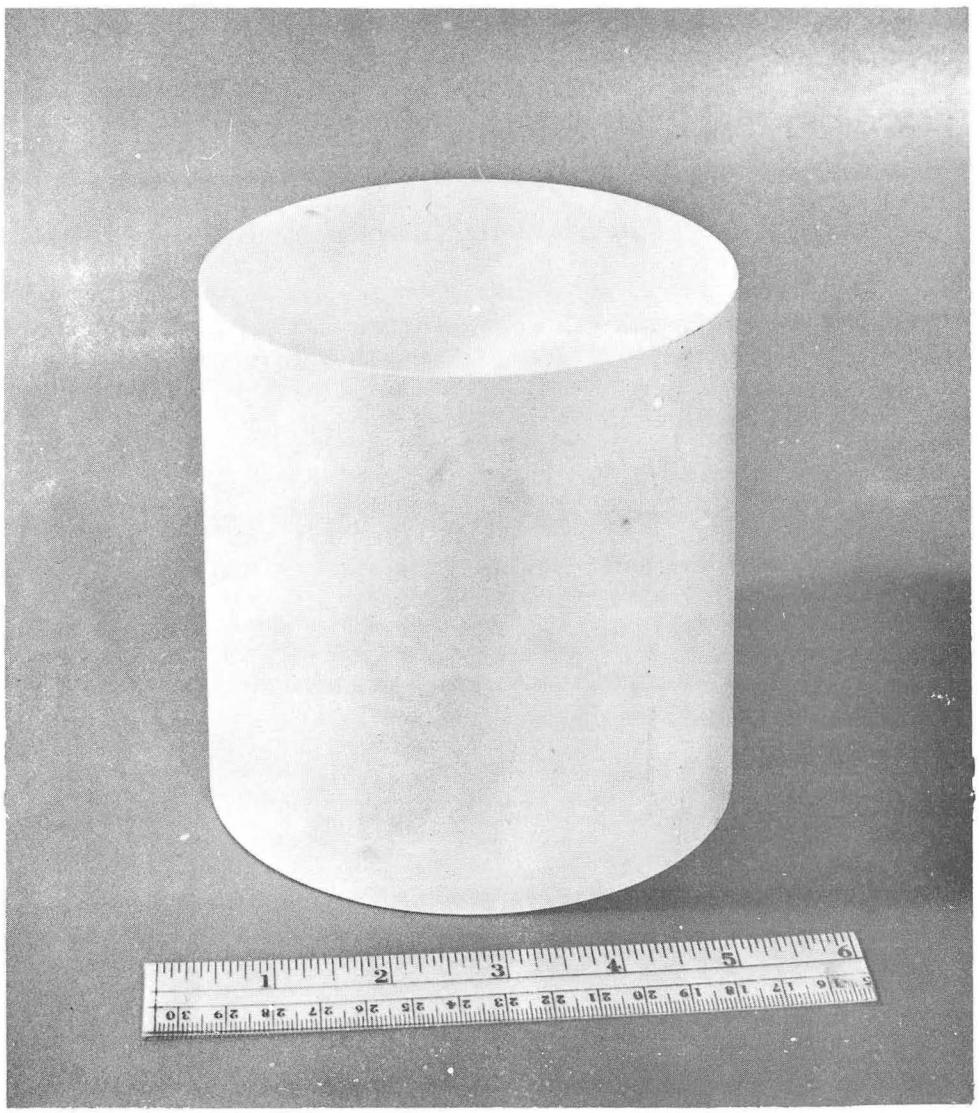

ZN-2141

Fig. 1. Plastic scintillator, 5×5 inches (1720 grams), used as the detector. Activity is induced directly in the scintillator material by (n, 2n) and (p, pn) reactions with carbon nuclei. Scintillator composition by weight: terphenyl, 2.5%, tetraphenylbutadiene, 0.02 to .03%; zinc stearate, 0.01%; polystyrene, ~ 97.5%.

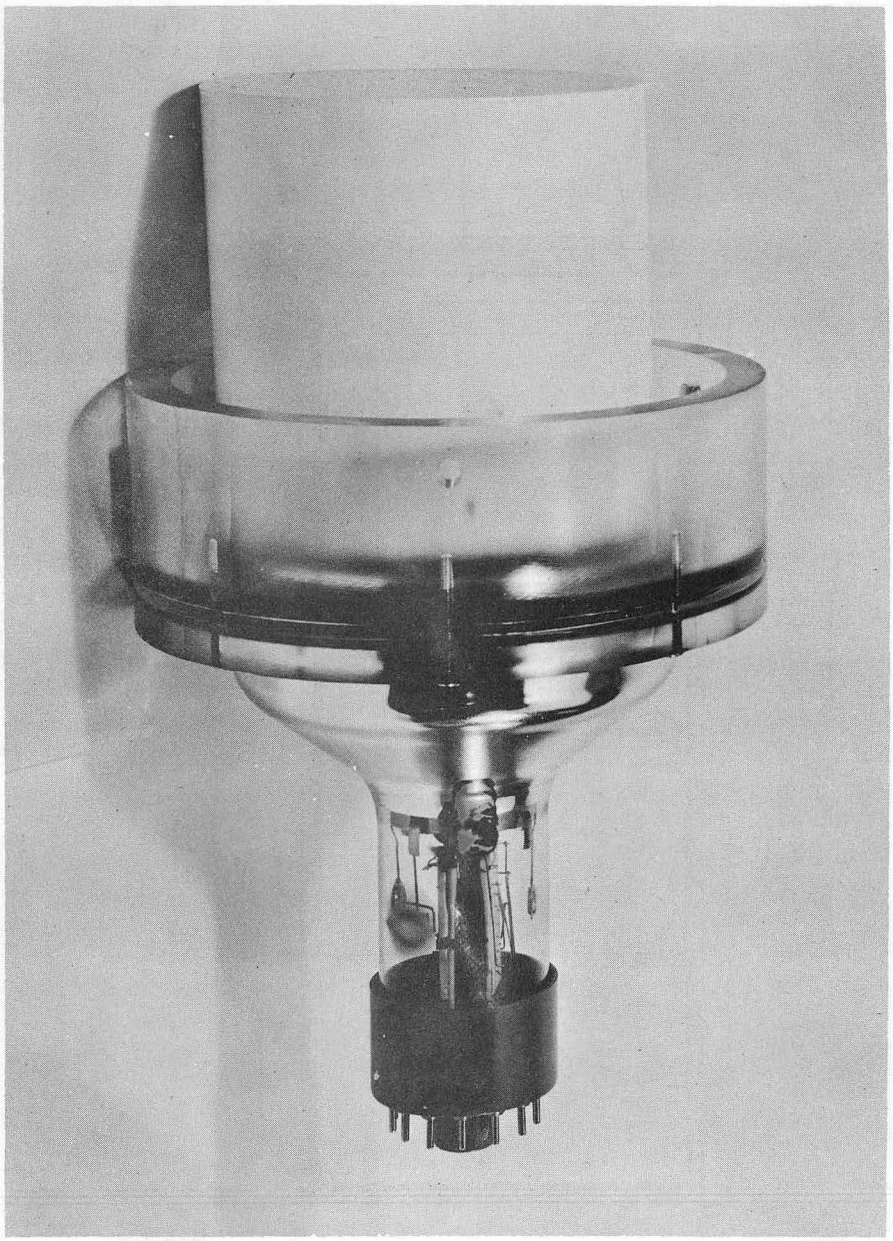

ZN-2143

Fig. 2. Scintillator placed in counting position inside a mineral oil bath with neoprene-gasketed Lucite container.

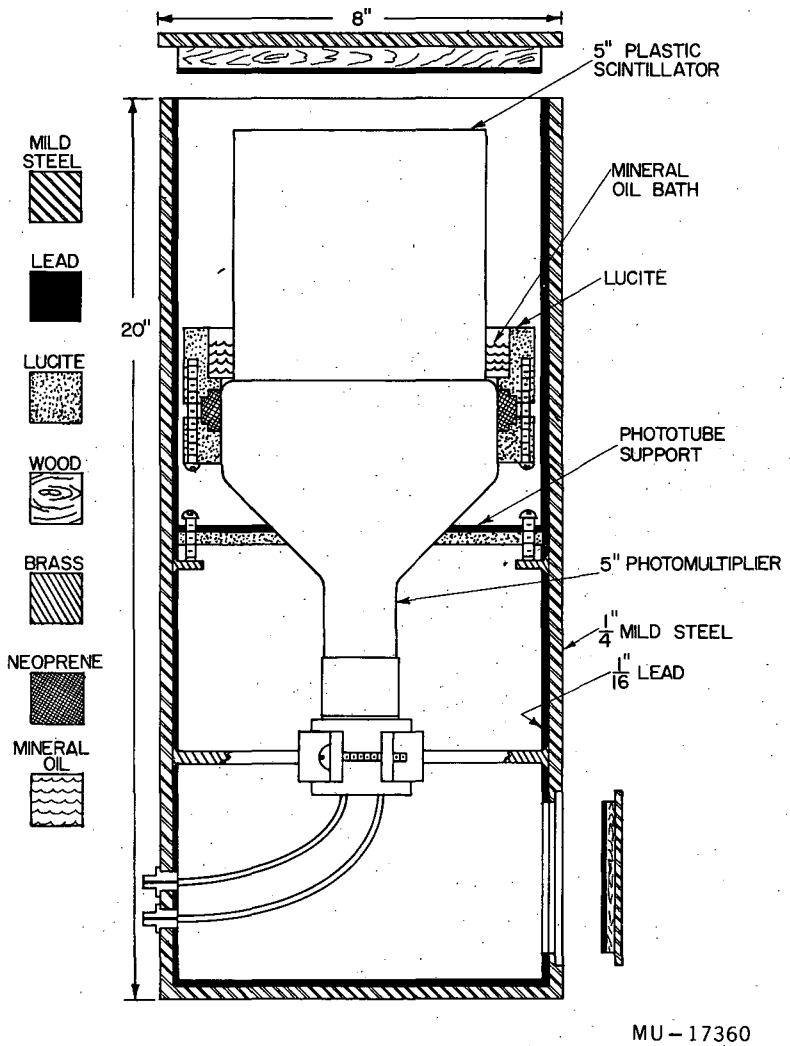

Fig. 3. Photomultiplier housing assembly, showing 1/4-inch mild steel sides, 1/16-inch lead liner, vertically mounted DuMont 6364 photomultiplier, and plastic scintillator immersed in mineral oil bath.

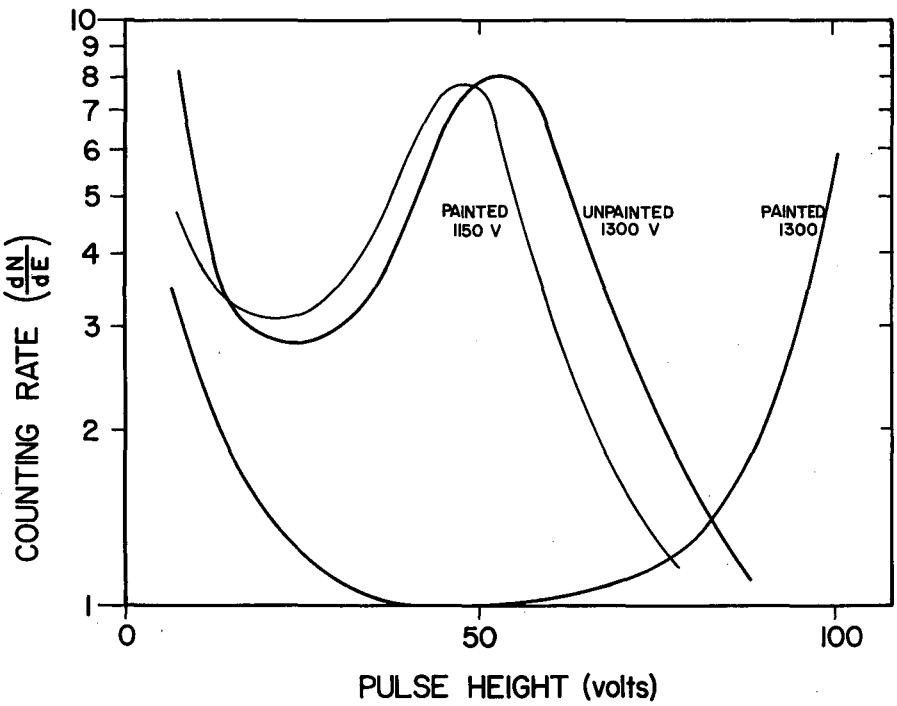

MU-17361

Fig. 4. The effective increase in gain provided by spraying the nonviewing surfaces of the scintillators with a white paint is clearly indicated. A Co^{60} source was used for obtaining the curves.

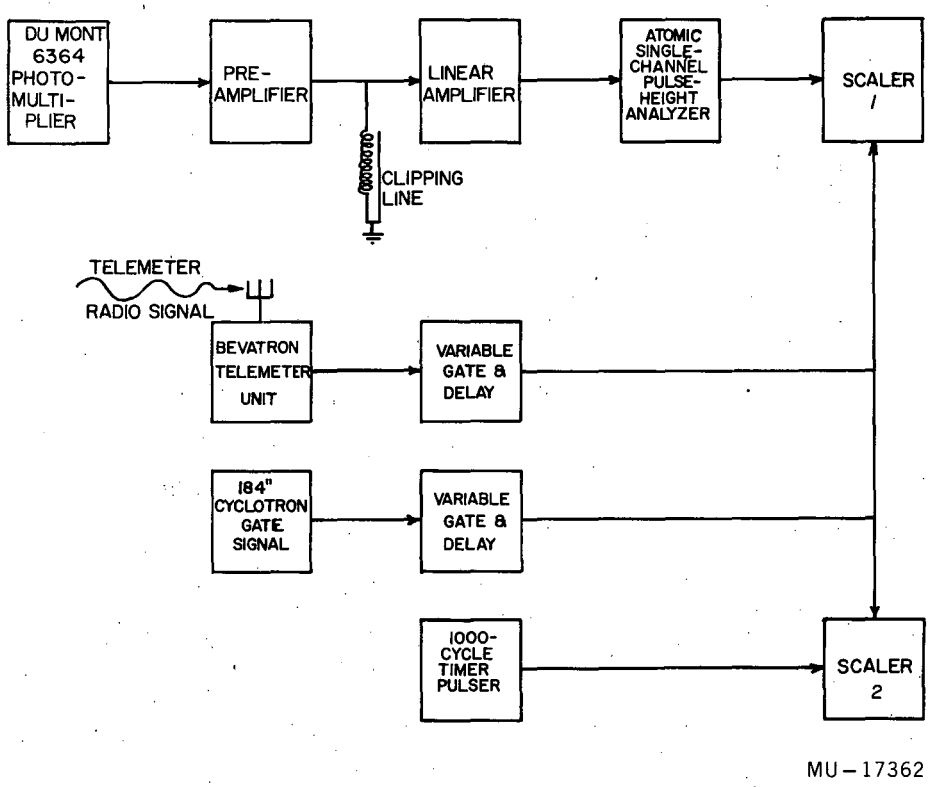

Fig. 5. Carbon-11 pulses from the photomultiplier are clipped, amplified, pulse-height analyzed, and counted in scaler No. 1 unless scaler No. 1 is gated off (as during the acceleration phases of the Bevatron and 184-inch cyclotron cycles). Scaler No. 2 is similarly gated and counts pulses from an accurate 1000-cycle generator, and thus is a measure of counting time.

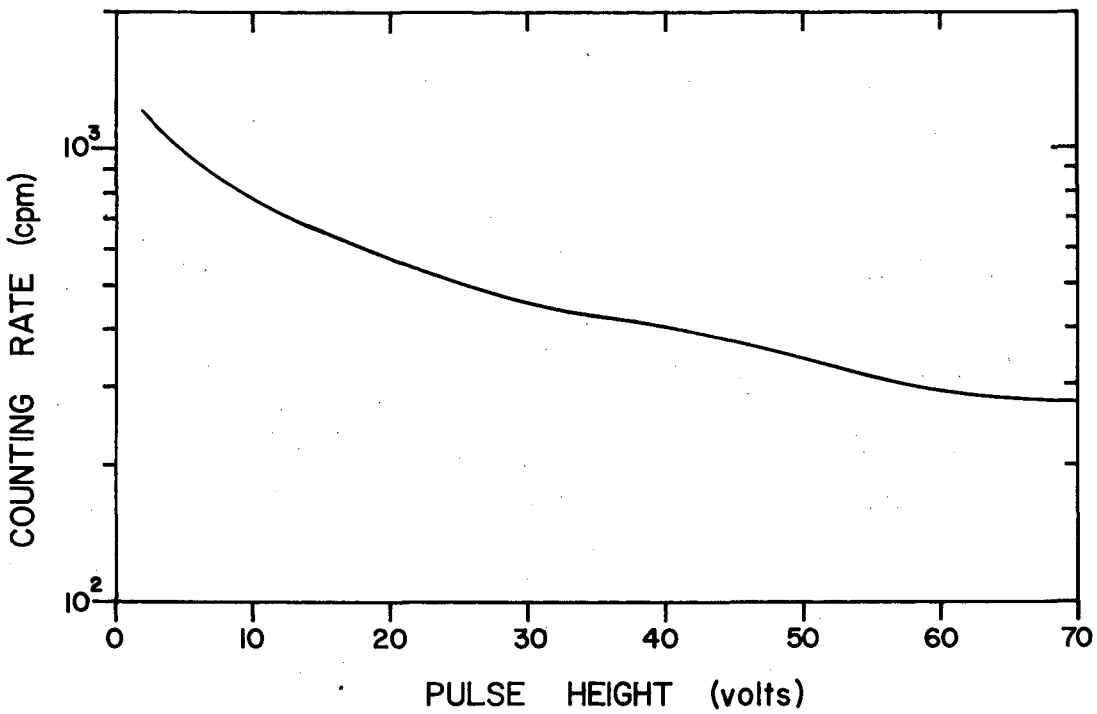

Fig. 6. Background integral with 4 inches of lead, and without the cosmic-ray anticoincidence shield.

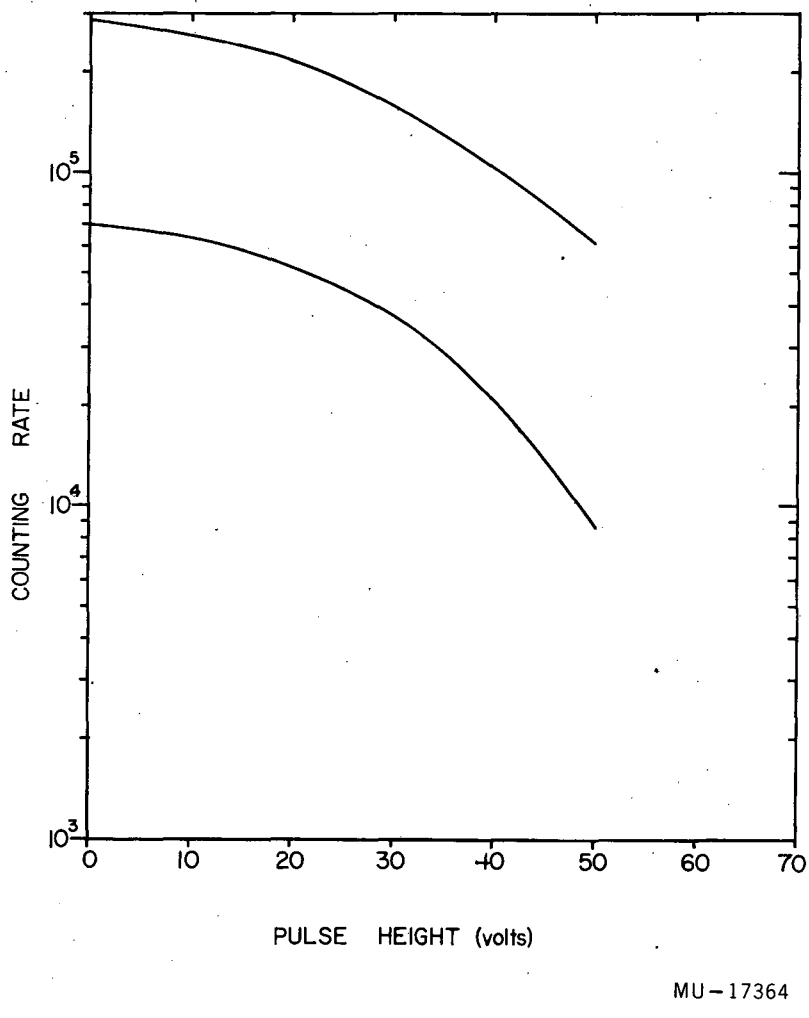

Fig. 7. Integral bias curves obtained at different beam intensities with two different scintillators indicate that no large errors are introduced by making the extrapolation from the 10-v operating point. Also, if many counts were being lost the curves would be more steep in this region. The similarity of the shapes of the curves indicates that corrections for individual scintillators are not necessary. For the two curves shown, the zero-bias correction factors are within 5% at 10 volts.

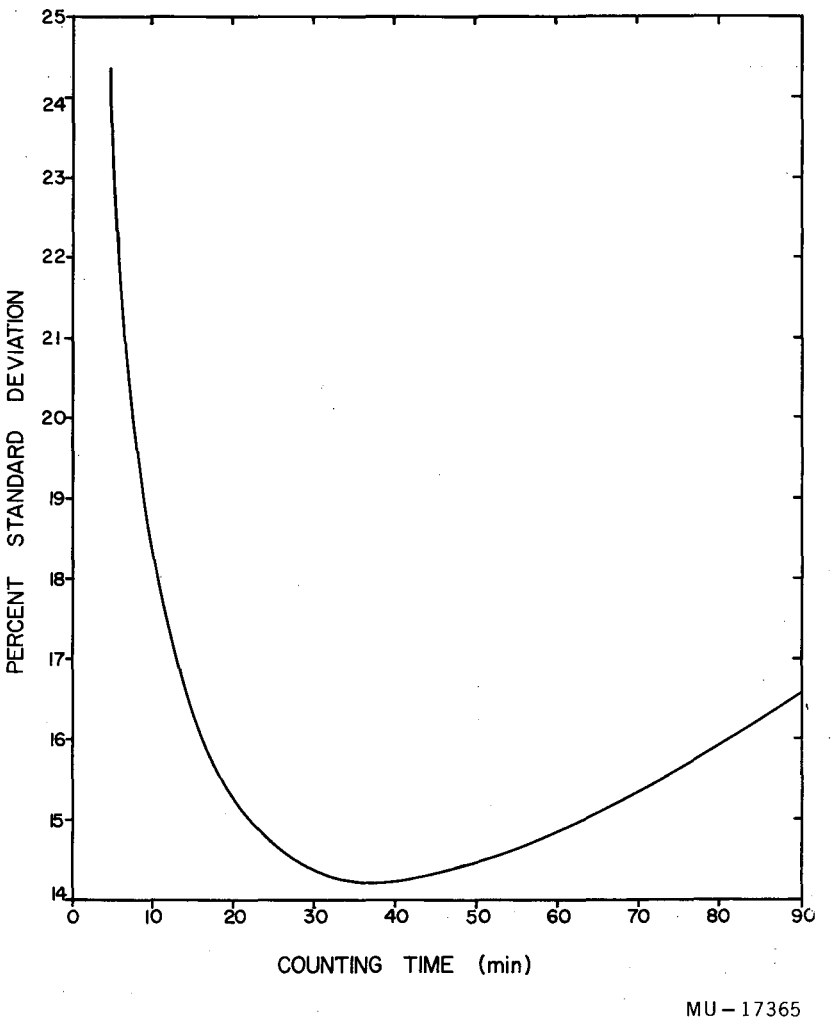

Fig. 8. A special case of Eq. (5), showing the error associated with the counting statistics as a function of the counting time for an incident flux density of 1 neutron cm^{-2} sec^{-1} for a scintillator irradiated to saturation, and including a 5-minute decay period prior to counting. For an optimum counting time of 38 minutes the standard deviation is less than 15%.

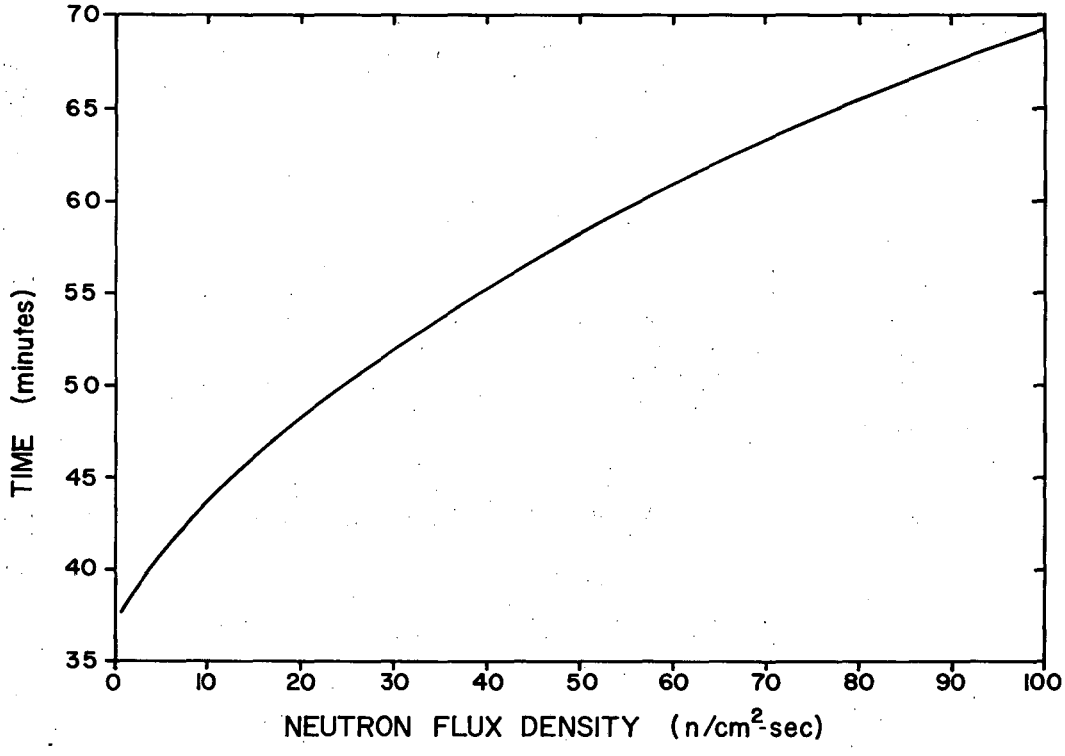

Fig. 9. Optimum counting times to provide minimum standard errors were calculated from Eq. (6) and are plotted as a function of the neutron flux density.

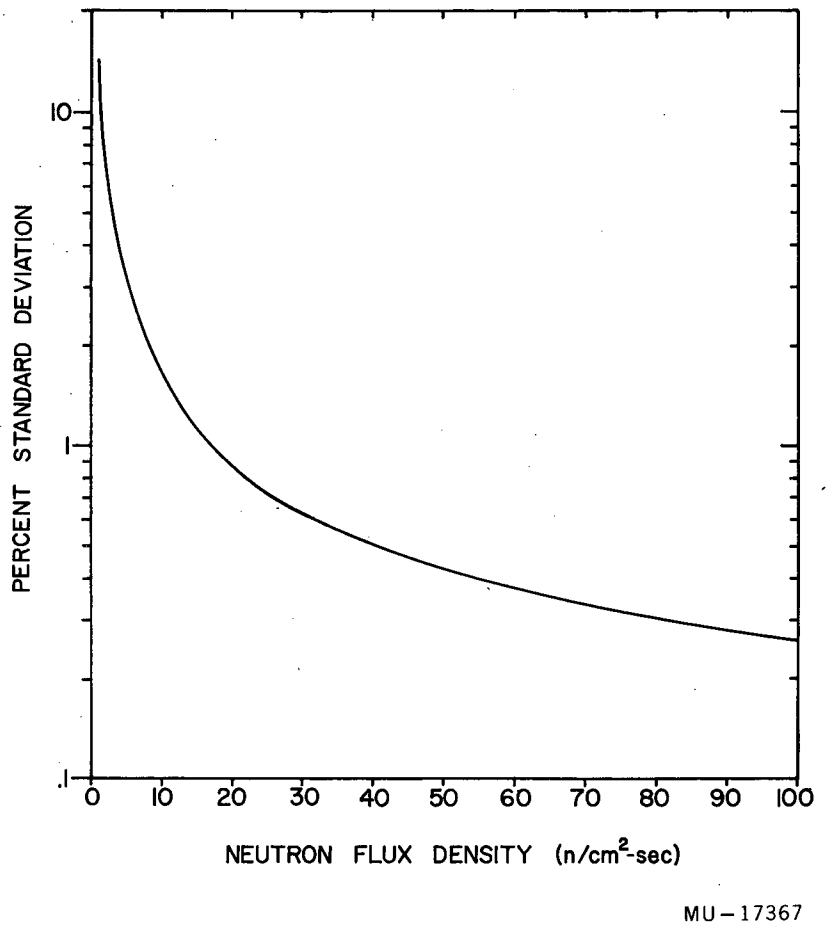

Fig. 10. The optimum counting times shown in Fig. 9 were substituted together with their associated flux densities, in Eq. (5), and their corresponding standard deviations plotted in Fig. 10. Thus a neutron flux density of 20 n $cm^{-2}sec^{-1}$ can be determined with a counting error less than 1% when a counting time of 48 minutes is used.

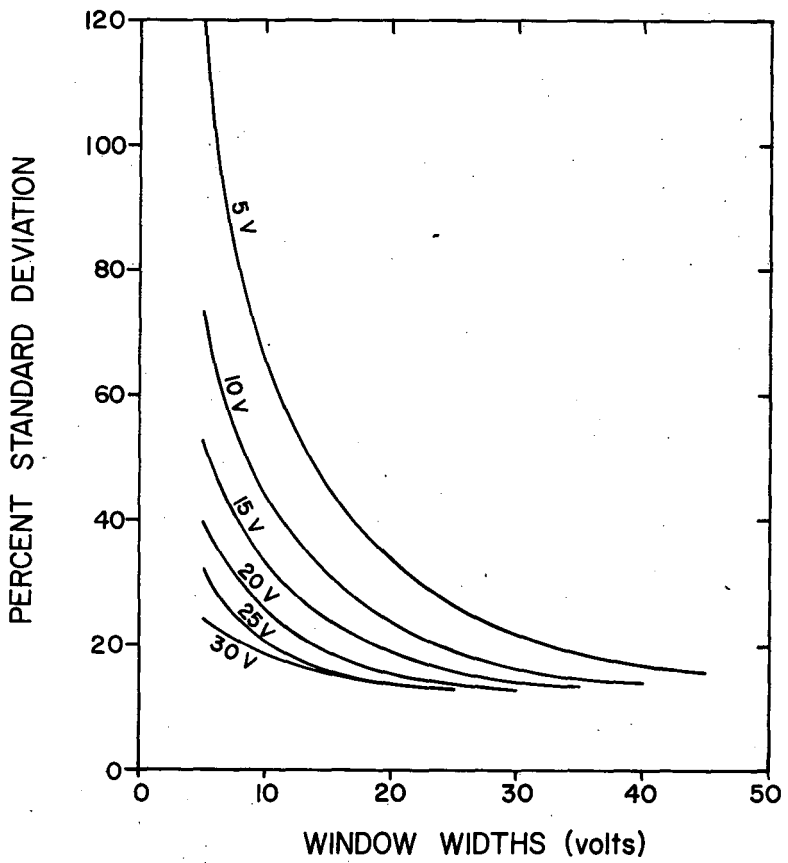

Fig. 11. Effective increase in sensitivity is obtained by adding an upper-level variable discriminator, thus taking advantage of the fact that the C^{11} integral bias curve falls off rapidly (Fig. 7) above about 25v while the background (Fig. 6) is still relatively flat above this region. With a bias of 20 volts and an upper-level discriminator of 50v (window width = 30v), the minimum standard deviation for 1 n $cm^{-2}sec^{-1}$ is 13%.

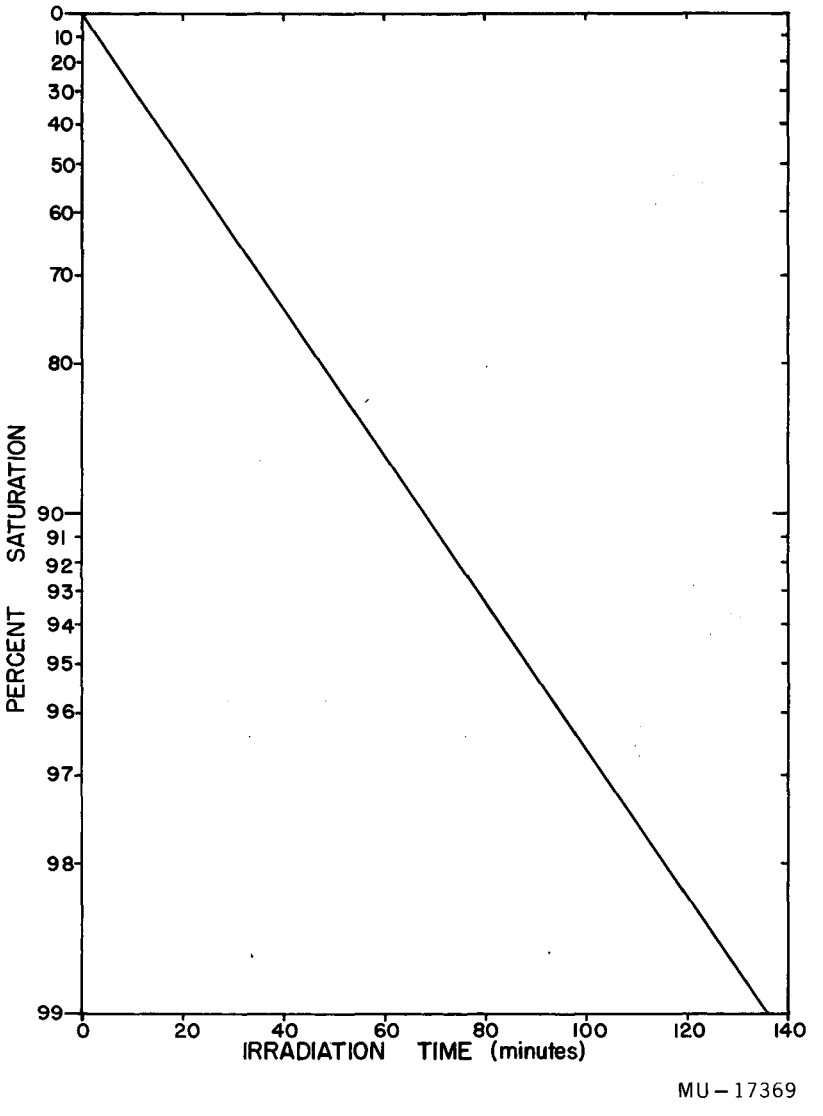

Fig. 12. Percent saturation shown as a function of irradiation time (to facilitate calculations involving irradiations other than those producing saturated activity).

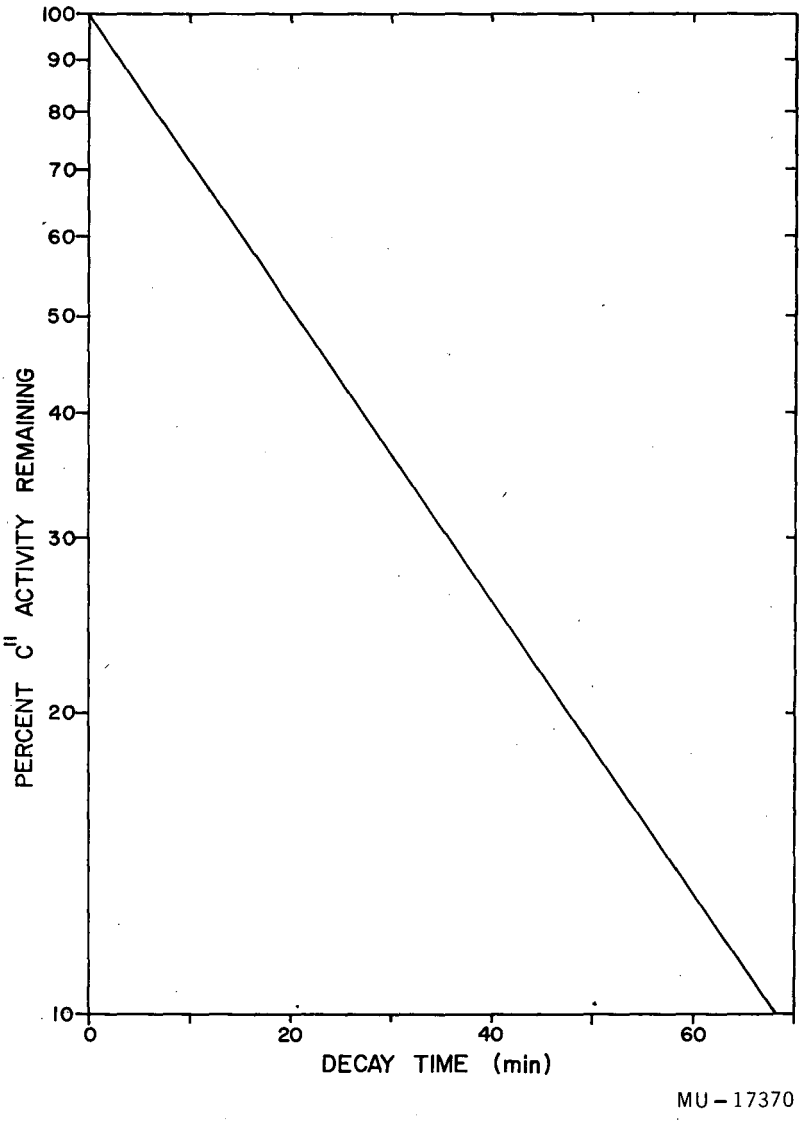

Fig. 13. A decay time (t_w) of 5 minutes, corresponding to about 85% of the activity remaining at the end of an irradiation, has been used in the calculations. Figure 13 may prove helpful when other values of t_w are employed.

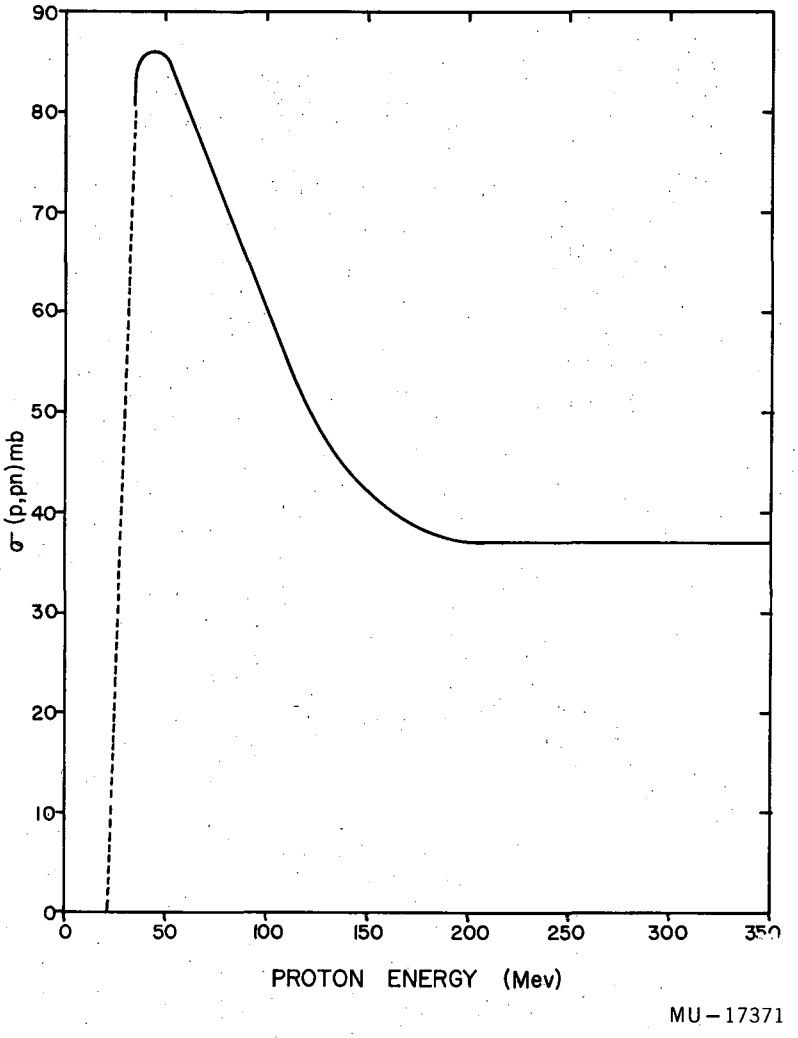

Fig. 14. $C_3^{12}(p, pn)C^{11}$ reaction cross sections taken from Crandall et al.[3]

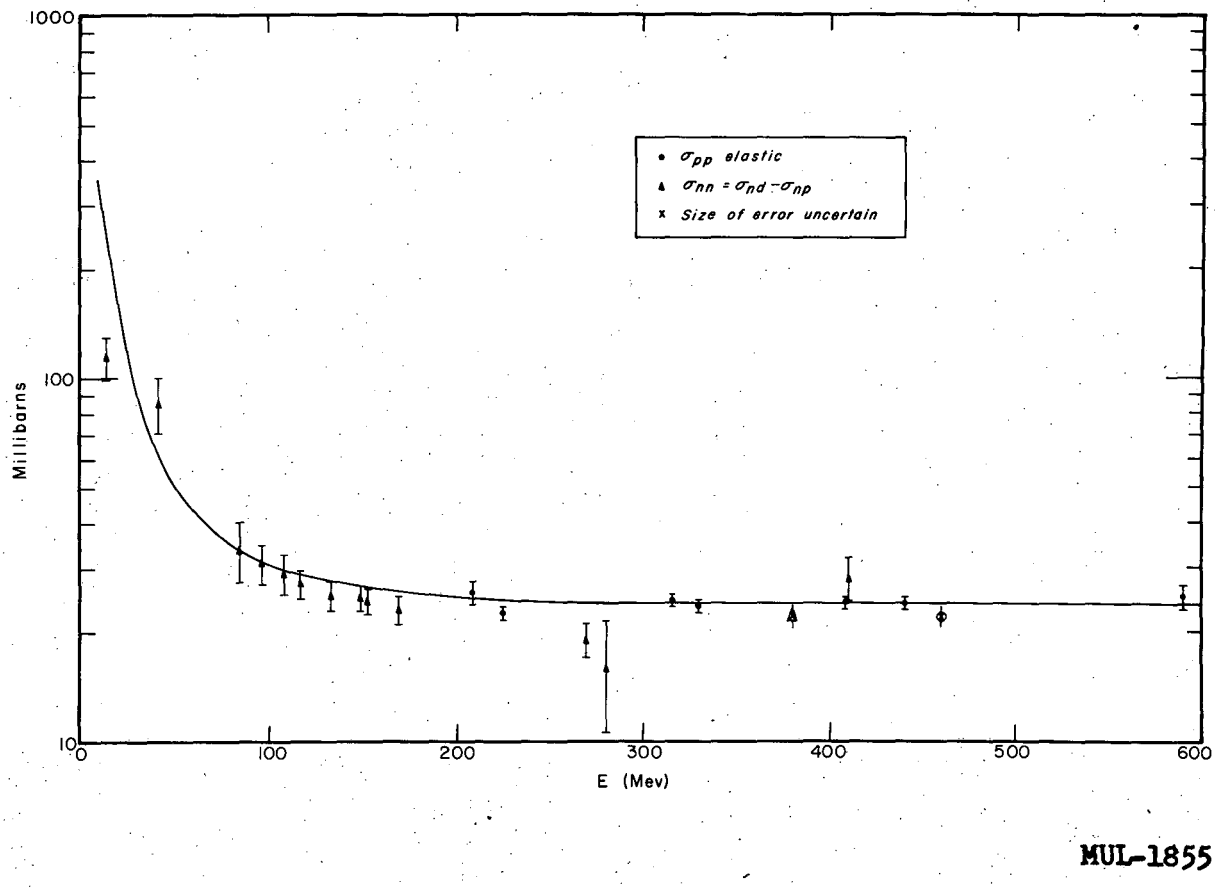

Fig. 15. Cross sections for (n, n) reactions (from Hess[4]). To be compared with (p, n) cross sections in Fig. 16.

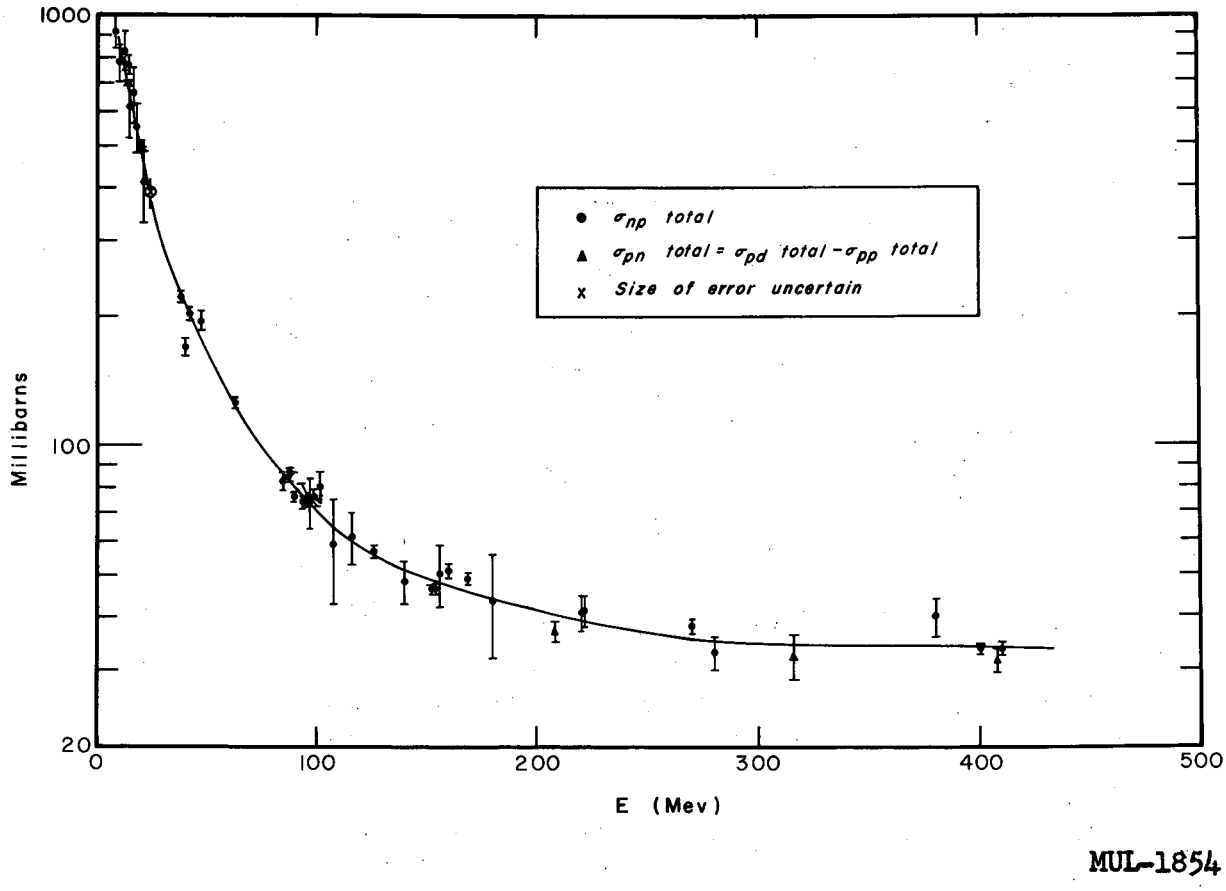

Fig. 16. Cross sections for (p, n) reactions (from Hess[4]). To be compared with (n, n) cross sections in Fig. 15.

Fig. 17. Threshold detector placed around the 4-1/2×4-1/2-inch NaI(Tl) crystal.

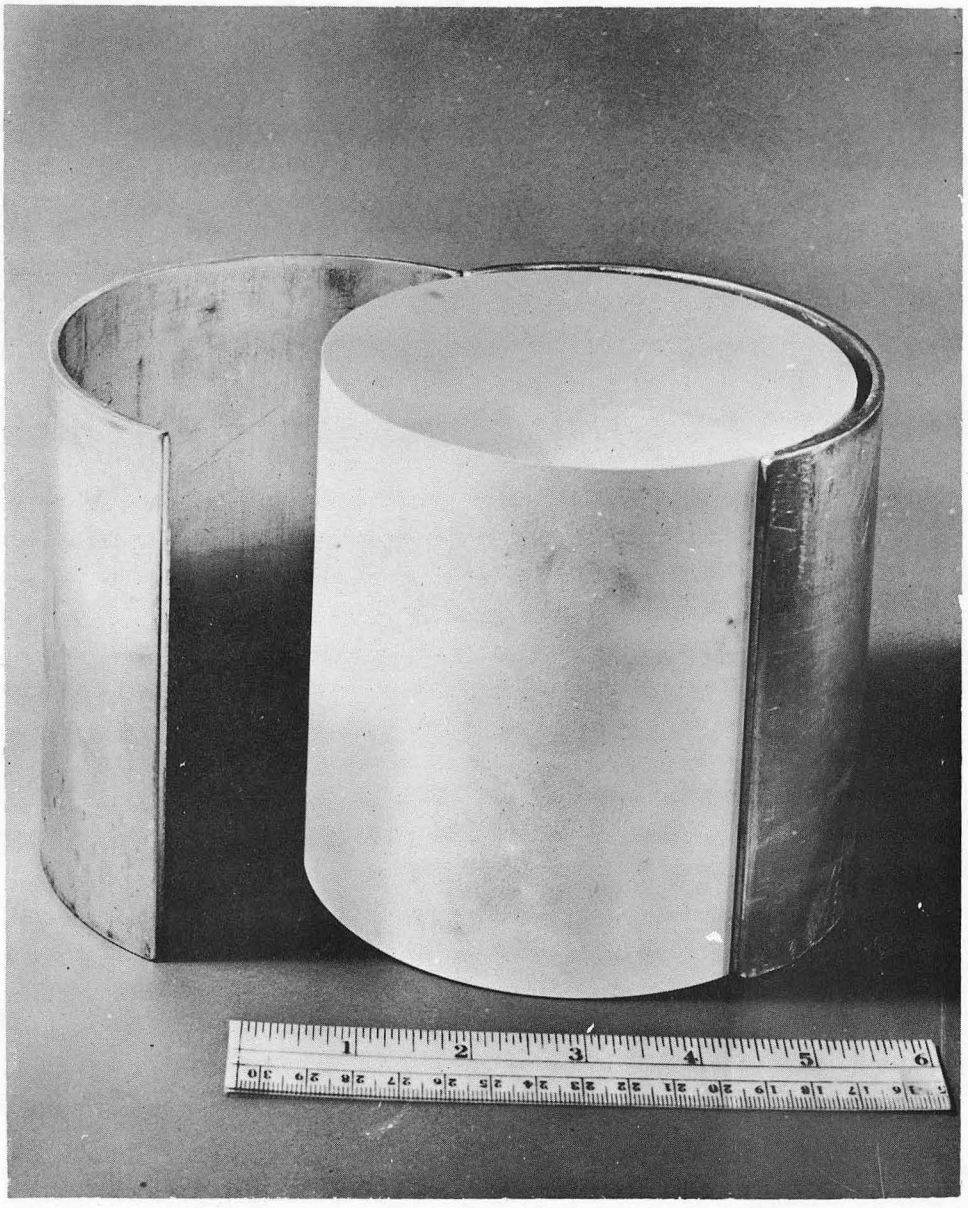

ZN-2142

Fig. 18. Threshold detector around one of the plastic scintillators.

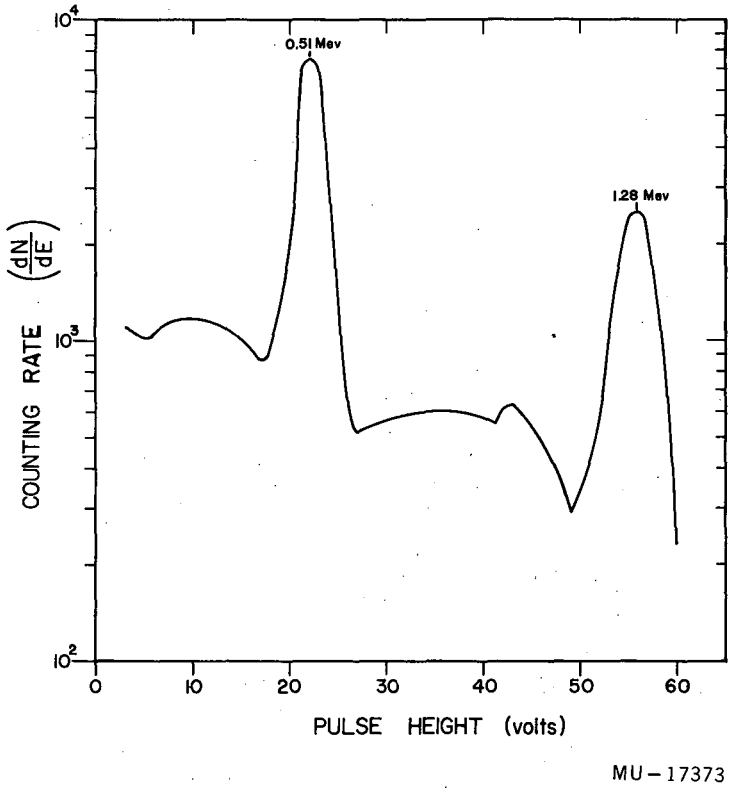

Fig. 19. Energy resolution with 3×3-inch NaI(Tl) crystal; the resolution (full width at half maximum) is 15% and 8% respectively at the two peaks.

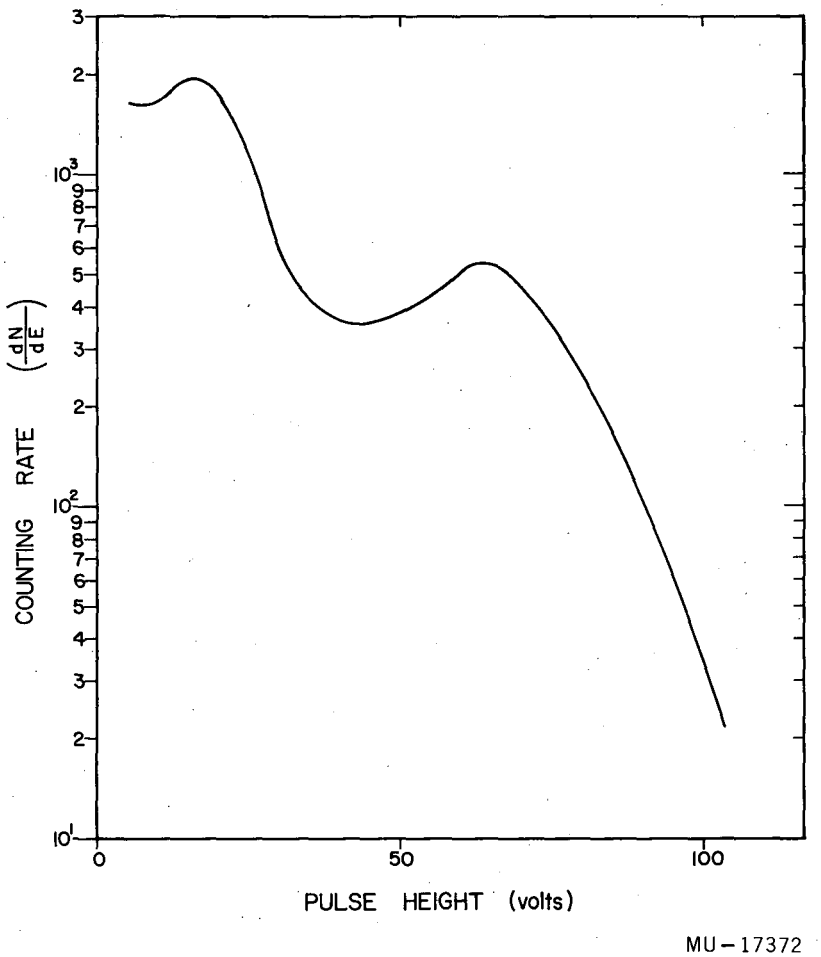

Fig. 20. Energy resolution for plastic scintillator with a Na^{22} source. Compare with Fig. 19.